Electronic Journal of Biotechnology 35 (2018) 18–24

Contents lists available at ScienceDirect

Electronic Journal of Biotechnology

Recombinant production and biochemical and *in silico* characterization of lactate dehydrogenase from *Geobacillus thermodenitrificans* DSM-465

Muhammad Shahid Nadeem *, Maryam A. Al-Ghamdi, Jalaluddin Azam Khan, Saida Sadath, Abdulaziz Al-Malki

Department of Biochemistry, Faculty of Science, Building A-90, King Abdulaziz University, Jeddah 21589, Saudi Arabia

ARTICLE INFO

Article history:
Received 19 February 2018
Accepted 23 June 2018
Available online 3 July 2018

Keywords:
Docking
Escherichia coli expression
Geobacillus thermodenitrificans
Glycolytic pathway
In silico studies
Inhibitors
Lactate dehydrogenase
Recombinant enzyme
Thermostable

ABSTRACT

Background: Lactate dehydrogenase (LDH) is an enzyme of glycolytic pathway, ubiquitously found in living organisms. Increased glycolysis and LDH activity are associated with many pathologic conditions including inflammation and cancer, thereby making the enzyme a suitable drug target. Studies on conserved structural and functional domains of LDH from various species reveal novel inhibitory molecules. Our study describes *Escherichia coli* production and characterization of a moderately thermostable LDH (LDH-GT) from *Geobacillus thermodenitrificans* DSM-465. An *in silico* 3D model of recombinant enzyme and molecular docking with a set of potential inhibitors are also described.

Results: The recombinant enzyme was overexpressed in *E. coli* and purified to electrophoretic homogeneity. The molecular weight of the enzyme determined by MALDI-TOF was 34,798.96 Da. It exhibited maximum activity at 65°C and pH 7.5 with a K_M value for pyruvate as 45 μM. LDH-GT and human LDH-A have only 35.6% identity in the amino acid sequence. On the contrary, comparison by *in silico* structural alignment reveals that LDH-GT monomer has approximately 80% identity to that of truncated LDH-A. The amino acids "GEHGD" as well as His^{179} and His^{193} in the active site are conserved. Docking studies have shown the binding free energy changes of potential inhibitors with LDH-A and LDH-GT ranging from −407.11 to −127.31 kJ mol^{-1}.

Conclusions: By highlighting the conserved structural and functional domains of LDH from two entirely different species, this study has graded potential inhibitory molecules on the basis of their binding affinities so that they can be applied for *in vivo* anticancer studies.

How to cite: Nadeem MS, Al-Ghamdi MA, Khan JA, et al. Recombinant production, biochemical and *in silico* characterization of lactate dehydrogenase from *Geobacillus thermodenitrificans* DSM-465. Electron J Biotechnol 2018;35. https://doi.org/10.1016/j.ejbt.2018.06.003.

1. Introduction

Lactate dehydrogenase (LDH; EC 1.1.1.27) is a glycolytic enzyme catalyzing the simultaneous interconversion of pyruvate and lactate [1]. Lactate is produced under hypoxic conditions by normal cells and under aerobic conditions by human cancer cells [2, 3]. Because of metabolic reprogramming, the lactate production is increased up to 40 times in cancer cells compared to that in normal cells [4]. Lactate is considered as an important energy fuel and a starting molecule for gluconeogenesis [5]. The increase in enzyme activity in malignant cells results in acidosis and pain. Hence, LDH inhibitors are considered as the key molecules for cancer treatment [6, 7]. LDH sensor strips have been introduced to replace the conventional plasma enzyme detection procedures [8]. Recently, LDH-based wearable biosensors have been introduced to detect lactate in the sweat to evaluate stress response and human performance [9]. Similarly, LDH-based glucose sensing cells are also applied in clinical investigations [10]. In addition to their clinical applications, such biosensors are also used for the detection of lactate in food and beverages [11]. LDH has been isolated and characterized from a wide range of organisms including animals, plants, and bacteria [12, 13]. Nucleotide sequences of DNA encoding the enzyme have been cloned and analyzed from a variety of organisms including mammals [14], bacteria [15], silkworm [16], and protozoans [17], and the characteristics of recombinant enzymes have also been studied.

In silico 3D structure determination and molecular docking techniques have been extensively applied to explore the affinities of small molecules in the binding site of targeted enzymes [18]. As an increasingly used bunch of tools and techniques in drug discovery, the binding specificity of small compounds against an enzyme can be estimated for applications *in vivo*. In case of target enzymes, the algorithms are applied to determine the inhibitory molecules with minimum binding energies [19]. During the last two decades,

* Corresponding author.
E-mail address: mhalim@kau.edu.sa (M.S. Nadeem).
Peer review under responsibility of Pontificia Universidad Católica de Valparaíso.

https://doi.org/10.1016/j.ejbt.2018.06.003

approximately 60 docking software and tools were introduced under different names, for commercial and academic applications [20,21]. The present study describes *Escherichia coli* expression, purification, and properties of L-LDH from *Geobacillus thermodenitrificans* DSM-465 (LDH-GT). We have demonstrated a 3D model for the recombinant enzyme that was further subjected to molecular docking studies against substrates, coenzymes, and potential inhibitors. The conservation of structural and functional residues was also analyzed by comparison with human LDH-A.

2. Materials and methods

2.1. Materials and chemicals for DNA manipulations

All the kits for PCR, DNA restriction, and ligation as well as chemicals and materials for cloning of recombinant plasmids, DNA isolation from agarose gel, plasmid isolation and purification, and characterization of recombinant enzyme were purchased from Sigma-Aldrich and Thermo Fisher. The genomic DNA of *Geobacillus* strain DSM-465 was obtained from DSMZ Germany. Modified bacterial strain (BL21 (DE3) codon plus RIL) and T7 promoter-based expression plasmid (pET21a (+)) were generously provided by the laboratories of the School of Biological Sciences, University of the Punjab, Lahore, Pakistan.

2.2. PCR amplification of the LDH-GT gene

The PCR amplification of the LDH gene was carried out using the primer sequences 5′-catatgaaaaacggaggaggaaacagag-3′ and 5′-ggatc cttactgcgcaaaggagc-3′. The restriction sites for *Nde*I and *BamH*I were introduced in the primer sequences to obtain the sticky ends along the complete open reading frame (ORF). The PCR reaction mixture consisted of 0.75 mM dNTPs; 1× *Taq* polymerase buffer containing KCl, 2.5 mM $MgCl_2$, and 2.5 U of *Taq* polymerase; 20 pM of each primer; and 2 μL of diluted DNA template with nuclease-free water, thus making a final volume of 25 μL. The thermocycler was initially adjusted for denaturation at 94°C for 4 min, followed by another denaturation step at 94°C for 40 s, annealing at 63°C for 1 min, and extension at 72°C for 1.5 min in the second step; these steps were repeated as 35 cycles. The final extension at 72°C for 25 min was carried out for the addition of poly-A sequence at the 3′-end of the amplified fragment.

2.3. Gene cloning and expression

The purified PCR product was ligated to the pTZ57R/T plasmid, and *E. coli* DH5α cells were transformed. Colonies successfully transformed with recombinant plasmids were selected initially by blue–white screening and further confirmed by the restriction analysis of isolated plasmids. The gene was cleaved from the pTZ57R/T plasmid using the restriction enzymes *Nde*I and *BamH*I and ligated to the pET21a(+) plasmid cleaved by the same pair of enzymes. The ligation mixture was used for the transformation of BL21 (DE3) RIL Codon plus cells according to the procedure provided in the InsTAclone kit (Thermo Fisher Inc., catalog no. K1213). A single colony of BL21 cells harboring the target gene was inoculated overnight in LB broth medium containing ampicillin (100 μg/mL). One percent inoculum from the above overnight culture was used for the growth of bacteria and incubated in an incubator shaker at 150 rpm and 37°C to attain an optical density of 0.1 at 600 nm wavelength; 0.2 mM isopropyl-β-D-thiogalactopyranoside (IPTG) was then added to the culture, and the culture was grown overnight at 20°C to induce gene expression.

2.4. Purification of recombinant enzyme

Bacterial cells were harvested by centrifugation and suspended in 45 mL of ice-cold 20 mM phosphate buffer, pH 7 (buffer A). The sample was sonicated in an ice box at moderate power for 10 min (2 min of rest followed after every 1 min of shock cycle). The homogenate was incubated at 70°C for 20 min followed by centrifugation at 12,000x *g* for 15 min at 4°C. The supernatant was precipitated using ice-cold acetone, and the precipitate was dissolved in buffer A and dialyzed overnight in 10 volumes of the same buffer at 4°C. Clear dialysate was obtained by centrifugation at 12,000 × g for 15 min at 4°C and subjected to a DEAE Sephadex column equilibrated with buffer A. The bound protein was eluted by a linear gradient of 0–0.5 M NaCl. Enzyme activity, specific activity, and other parameters were recorded at each purification step and tabulated.

2.5. Molecular weight of recombinant LDH

The purity and molecular weight of the recombinant enzyme were determined by 15% SDS-PAGE [22] and MALDI-TOF analysis. Two microliters of the purified recombinant enzyme solution (2 μg/μL) was mixed with 20 μL of matrix-B (5 mg of sinapinic acid in 1 mL of 35% acetonitrile containing 0.15% trifluroacetic acid [TFA]), and 6 μL of this mixture was spotted on a mass spectrometric plate, and the spot was air dried for 30–40 min. The spectrum was recorded with Bruker Autoflex MALDI-TOF (Bruker Daltonics Inc., Billerica, MAUSA).

2.6. Enzyme kinetics

The K_M value for pyruvate was determined by generating a Lineweaver–Burk double reciprocal plot by using a linear increase in substrate concentration, starting from 5 to 320 μM. The reaction consisted of 280 μM of NADH prepared in phosphate buffer, pH 7.0. The reaction mixture was adjusted at different temperatures to find out the optimum temperature for enzyme activity. Temperature stability of the enzyme was determined by incubating the enzyme sample at 40, 50, 60, 70, 80, and 90°C for 5 min followed by enzyme assay. Enzyme activity was also measured by using the reaction mixture adjusted at pH ranging from 4.0 to 8.5 to determine the optimum pH.

2.7. In silico protein modeling and validation

As the protein structure of LDH-GTD (LDH of *G. thermodenitrificans* DSM-465) was unavailable at protein database bank (PDB) server, we

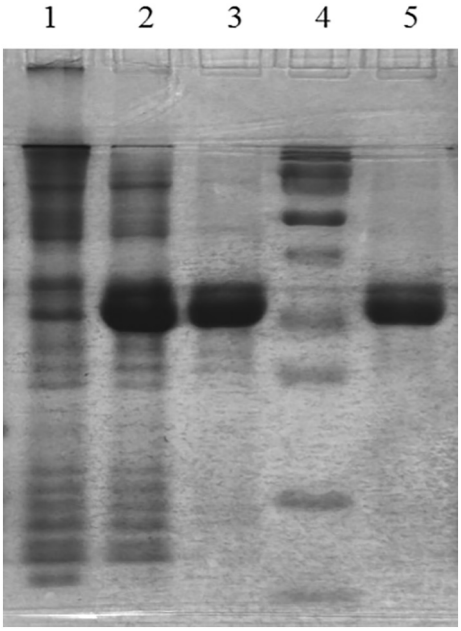

Fig. 1. Image of SDS-PAGE. Lane 1: Negative control, induced pET21a (+) proteins in *E. coli*, Lane 2: Induced pET21-GT proteins, Lane 3: Selective precipitate after heat treatment, Lane 4: Protein marker (Thermo Fisher catalog no. 26616), Lane 5: Purified LDH.

Table 1
Purification steps and related activity, specific activity, percentage yield, and fold purification for recombinant LDH-GT. In total, 45 mL of cellular extract was processed after sonication and 6.5 mL of the purified sample was obtained.

Purification stages	Activity (U/mL)	Protein content (mg/mL)	Specific activity (U/mg)	Total units	Percentage recovery	Fold purification
Sonicated extract	294	18.5	15.89	13,230	100	1
Heat treated/selective precipitated	832	3.21	259.2	8320	62.88	16.31
DEAE-Sephadex column	780	2.0	390	5070	38.32	24.54

generated a 3D model by Swiss-Model [23] and I-TASSER [24] servers *by* employing the crystal structure "1LDN" (LDH protein crystal structure of *Geobacillus stearothermophilus*) as a template. Subsequently, the quality of the predicted model was examined by using RAMPAGE, a protein structure validation server [25] that validates the results in terms of phi, psi, and Cbeta deviations by generating a Ramachandran plot for the protein built.

2.8. Molecular docking and comparative analysis

The 3D structures of selected potential inhibitors [26] were retrieved from chemical structure databases like PubChem and ChemSpider servers and were subjected to docking against the LDH-GT protein using Hex docking server [27]. Free energy changes (ΔG values) for the establishment of each docked protein–inhibitor complex were recorded to rank the inhibitors for binding affinities. The same set of inhibitors was again docked against the human LDH-A (4ZVV) protein to make a comparative analysis. Initial inhibitors present in the 4ZVV complex structure were removed manually to avoid docking error with desired selected inhibitors. Moreover, a region of 300 residues of LDH-GT and LDH-A was structurally aligned by using PyMOL for the analysis of conserved structural and functional regions; ConSurf web server [28,29] identified and compared the evolutionary conserved residues.

3. Results

3.1. PCR amplification and molecular cloning of the LDH-GT gene

A 954-bp gene sequence coding for the *G. thermodenitrificans* LDH gene was amplified by PCR and T/A cloned using the pTZ57R/T plasmid. The recombinant plasmid pET21-LDHGT was constructed by the ligation of the LDH gene cleaved from the pTZ57R/T plasmid by using the restriction enzymes *Nde*I and *BamH*I. Competent cells of BL21 (DE3) RIL Codon (+) strain of *E. coli* were transformed by the plasmid pET-LDHGT. The transformed cells were confirmed by restriction analysis of isolated plasmid.

3.2. Expression, purification, and initial characterization

The soluble and active enzyme was induced by 0.2 mM IPTG overnight at 20°C; cells were then harvested and sonicated to break the bacterial cell wall, and the proteins were analyzed by SDS-PAGE (Fig. 1). The proteins expressed included approximately 50% of total *E. coli* proteins. The recombinant enzyme was purified by selective heat denaturation and acetone precipitation followed by dialysis and DEAE-column-based anion exchange chromatography. The percentage recovery of the purified enzyme was 38.32%, and the specific activity was 390 U/mg; the enzyme was purified to 24.54-fold (Table 1). On SDS-PAGE, the molecular weight of the enzyme was approximately 35 kDa (Fig. 1), and it was determined as 34,798.96 Da by MALDI-TOF analysis (Fig. 2).

3.3. Kinetic properties of LDH-GT

The purified recombinant enzyme exhibited maximum activity at 65°C, and it retained half activity when incubated at 85°C for 10 min. Although it was active under a wide pH range, the optimum pH for enzyme activity was 7.5. The K_M was calculated as 45 μM of pyruvate (Supplementary figures and tables).

3.4. In silico modeling and validation

Swiss-Model generated the LDH-GT models in both forms, *i.e.*, monomer and homotetramer. Homotetramer (Fig. 3) was opted for further study for visualization by PyMOL Molecular Graphics System,

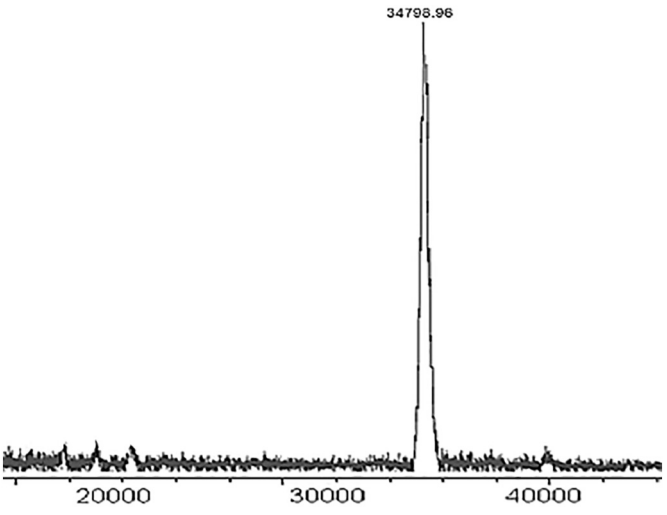

Fig. 2. Molecular weight of purified lactate dehydrogenase (34,798.96 Da) as determined by MALDI-TOF analysis. X-axis indicates the protein molecular weight (Daltons), and the Y-axis indicates the intensity of laser beam.

Fig. 3. A 3D model of the LDH-GT (*Geobacillus thermodenitrificans* – DSM-465) protein in a homotetrameric form represented as cartoons: Chain A: Brown; Chain B: Violet; Chain C: Green; Chain D: Red (Visualized by Chimera).

Version 1.2r3pre. The data reveal that the template-based structure of LDH-GT built is of highly excellent quality and stability (Fig. 4; Table 2) probably because of the fact that the template crystal model (1LDN) contained equal number of residues (317) in its protein sequence, which are structurally >96% identical to that of LDH-GT.

3.5. Molecular docking and comparison with human LDH-A

Molecular docking results revealed that NADH and 1E4 are the most significant inhibitors of LDH enzymes of both *Geobacillus* and *Homo sapiens* origin, as indicated by the calculated binding free energies (Table 3). The structural comparison by superimposition revealed that, although the sequence of LDH-GT and human LDH-A have less than 36% similarity, the LDH-GT monomer region is 80% structurally identical to the LDH-A monomer region (Fig. 5). The selected interacting partners are represented as sticks in Fig. 6. ConSurf webserver exhibited conservation, *i.e.*, the exposed and buried states of the residues (Fig. 7A). The continuous conservation scores are divided into a discrete scale of nine grades for visualization, from the most variable positions grading 1 (turquoise color), through intermediately conserved positions grading 5 (white color), to the most conserved positions grading 9 (maroon color) (Fig. 7B). Our studies have shown a noticeable conservation of residues at spatial structural and functional positions.

4. Discussion

Enzymes are important targets in disease control strategies. Conserved structural and functional domains provide hotspots for the selection or designing of potent and broad-spectrum enzyme inhibitors [30,31,32]. Herein, we report *E. coli* expression, purification, and biochemical and *in silico* characterization of a moderately thermostable LDH from an unexplored *Geobacillus* strain. Further, we made a comparative analysis of our recombinant enzyme with human LDH-A by molecular docking to identify evolutionarily conserved structural/functional domains and to determine their interaction with some potential inhibitors. A 954 bp gene sequence encoding 317 amino acids was expressed in BL21 (DE3) strain of *E. coli* using T7 promoter-based pET21a (+) plasmid vector. Expression of the soluble, active enzyme was obtained at low IPTG concentration and low temperature conditions. Similar *E. coli* expression conditions have been reported in

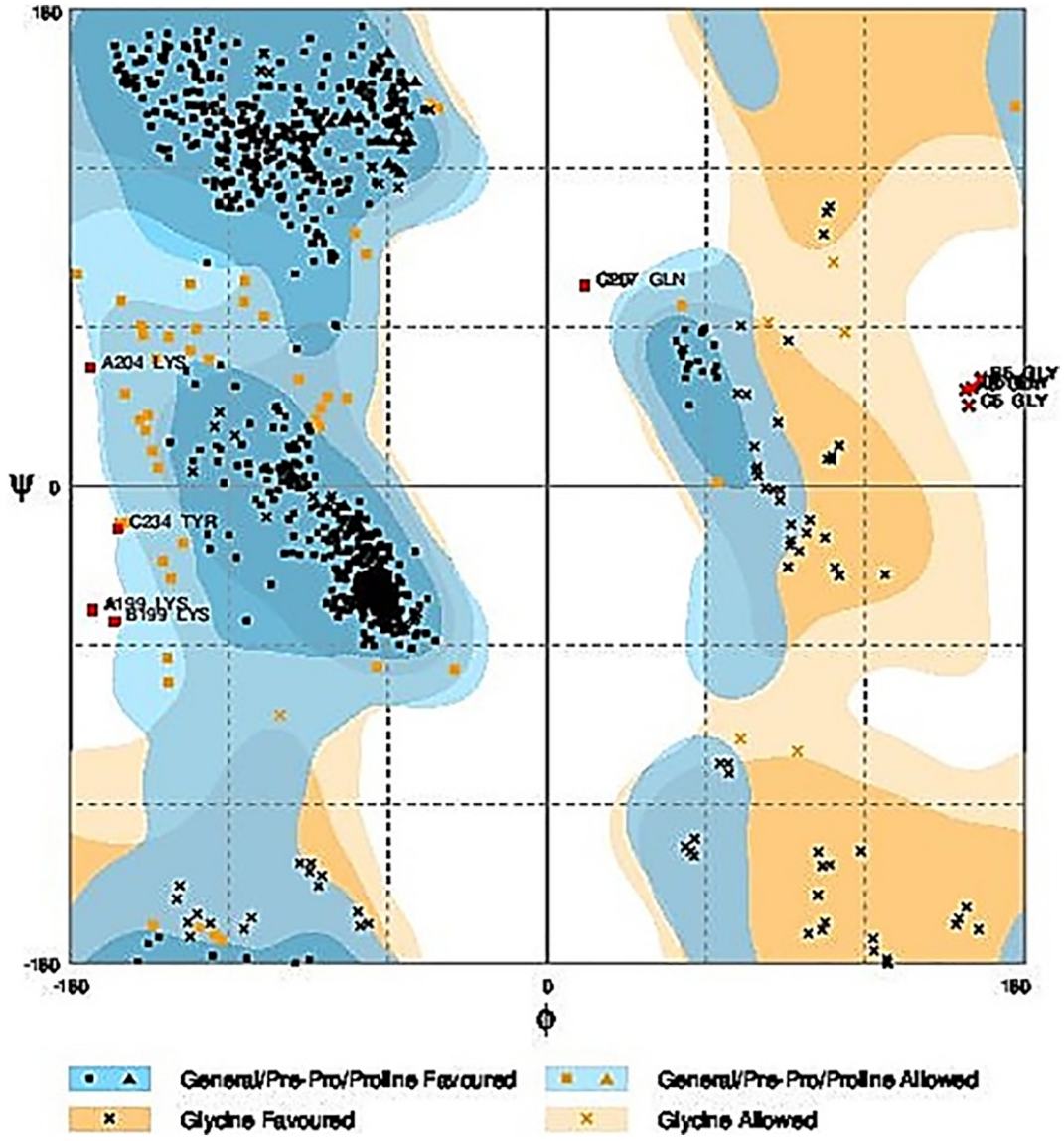

Fig. 4. The Ramachandran Plot generated by the RAMPAGE server depicting the quality of the 3D model of the LDH-GT enzyme. The plot along with I-TASSER values (Table 2) validated the accuracy of the homotetrameric model.

Table 2
3D protein model quality evaluations from I-TASSER.

Protein	C-score[a]	TM score[b]	RMSD[c]	IDEN[d]	Cov[e]
LDH	0.710	0.980	0.99 Å	0.877	0.997

[a] Confidence (C) score for estimating the quality of predicted models (range − 5 to 2).
[b] Template Modeling score (TM score) measures the structural similarity between two structures; TM score > 0.5 indicates a model of correct topology and a TM score < 0.17 means a random similarity range from 0 to 1.
[c] Root Mean Square Deviation (RMSD) of heavy atoms with regard to the experimental structure.
[d] IDEN is the percentage sequence identity in the structurally aligned region (range 0 to 1).
[e] Cov represents the coverage of global structural alignment and is equal to the number of structurally aligned residues divided by the length of the query protein cluster (range 0 to 1).

Fig. 5. LDH-GT monomer (orange) and LDHA monomer (green) superimposed for comparative structural analysis.

recent literature [33,34]. Efficiently expressed enzyme was purified by selective heat denaturation followed by precipitation and ion exchange chromatography and analyzed by SDS-PAGE (Fig. 1). It was purified up to 24.54-fold, with 38.32% recovery and 390 U per milligram specific activity (Table 1). The molecular weight of recombinant enzyme was 34,798.96 Da as determined by MALDI-TOF analysis (Fig. 2). Estimated molecular weight was similar to the theoretical molecular weight (34,828.56 Da) calculated by ProtParam software. Similar molecular weight of LDH (34 kDa) from *Staphylococcus aureus* has been reported [35]. However, a slightly higher range of molecular weights, *i.e.*, 36,464.3 Da, 36,557.5 Da, 36,530.21 Da, and 36,052.9 Da, was found in eukaryotic species [14, 36, 37]. An optimum temperature of 65°C and stability up to 85°C indicate that the enzyme falls in the moderately thermostable range. Similar temperature stability has been reported from *Clostridium thermocellum* [38]. However, the enzyme described in the present study has reasonably higher stability than mammalian LDH [14, 36]. The K_M value for pyruvate (45 μM) obtained in our study is less than those for pyruvate reported in human normal and tumor cells (63 and 78 μM, respectively), thus indicating the better affinity of the enzyme with the substrate [39]. *In silico*-generated 3D model of LDH-GT indicates its existence as a homotetramer (Fig. 3). The Swiss-Model [40] and PyMol Molecular Graphics version 1.2r3pre [41] were used for the construction, visualization, and analysis of the enzyme structure. These software programs are being applied in recent studies to determine the structure and function of enzymes [42]. The 3D model of LDH-GT built was of higher quality as evaluated by online I-TASSER [24] and Ramachandran Plot generated by the RAMPAGE server (Fig. 4; Table 2). Recent studies have applied these software programs [23,43]. Although there was only 35.6% amino acid identity between LDH-GT and LDH-A, comparative analysis has revealed approximately 80% identity in 3D model structures of their monomers (Fig. 5). The results indicate a conserved identity of structure and function out of diversity of amino acid sequence. The binding pocket for pyruvate and NADH has been determined by molecular docking complexes (Fig. 6). We evaluated several potential inhibitory interacting molecules by molecular docking, and NADH, IE4, IE7, 2B4, NIH2, and FX11 have shown the highest binding free energy change for both LDH-A and LDH-GT (Table 3). Our findings are also supported by similar studies [26]. We enlisted the LDH-GT and LDH-A inhibitors rank wise; this rank will be further used to develop a novel inhibitor against LDHs. A detailed analysis of conserved structural and functional amino acids was also conducted in our investigation. On protein surfaces, there are amino acids involved in binding and catalysis, and these amino acids are often evolutionarily conserved [28]. Following this principle, ConSurf analysis [29] has identified a batch of five amino acids "GEHGD" in the LDH-GT protein sequence; these amino acids are conserved in the human LDH-A protein sequence that serves as a putative binding site for substrate and inhibitors, as they are quite conserved and in an exposed state (except Gly^{177}, which is in the buried state). His^{179} in LDG-GT might have a binding function same as that of His^{193} in LDH-A (Fig. 7A). In the ConSurf output data, the values for conserved and variable amino acids are indicated by different colors (Fig. 7B).

5. Conclusions

Our study describes the cloning, *E. coli* expression, and biochemical characterization of LDH from a new *Geobacillus* species. A 3D model of the recombinant enzyme was built, validated, and compared *in silico* with that of human LDH-A. By highlighting the conserved structural and functional domains including the active site residues, we ranked

Table 3
Binding free energies of the LDH–inhibitor docked complexes of *Geobacillus thermodenitrificans* DSM-465 and *Homo sapiens.*

Protein	Inhibitor	ΔG (kJ mole^{-1})	Rank	Protein	Inhibitor	ΔG (kJ mole^{-1})
LDH-*Geobacillus thermodenitrificans* DSM-465	NADH	−383.29	1	LDH-A *Homo sapiens*	1E4	−407.11
	1E4	−380.34	2		NADH	−357.56
	1E7	−289.53	3		2B4	−310.02
	NIH 2	−269.14	4		1E7	−308.6
	FX11	−262.51	5		NIH 2	−296.36
	2B4	−252.22	6		FX11	−271.27
	GALLOFLAVIN	−218.41	7		6P3	−228.08
	AJ1	−216.28	8		GALLOFLAVIN	−222.37
	6P3	−198.66	9		AJ1	−198.55
	PYR	−127.31	10		PYR	−135.5

Note: ΔG represents binding free energies of docked complex of respective protein and inhibitor.

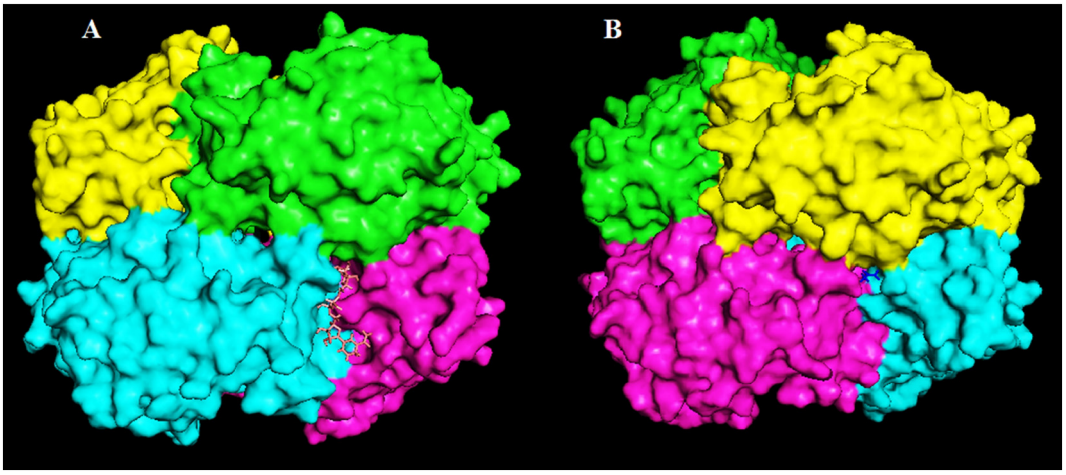

Fig. 6. Docked complex (ES) exhibiting LDH-GT homotetramer chains in the surface view and the substrates/co-factors in sticks. **A** – Docking complex of LDH-GT and NADH, **B** – Docking complex of LDH-GT and Pyruvate. Chain A – green; Chain B – Cyan; Chain C – Magenta; Chain D – Yellow.

several inhibitors by calculating the binding free energy changes with several protein partners. Findings can be prolonged for the selection and application of inhibitor molecules in anticancer research.

Conflict of interest

The authors declare no conflict of interest.

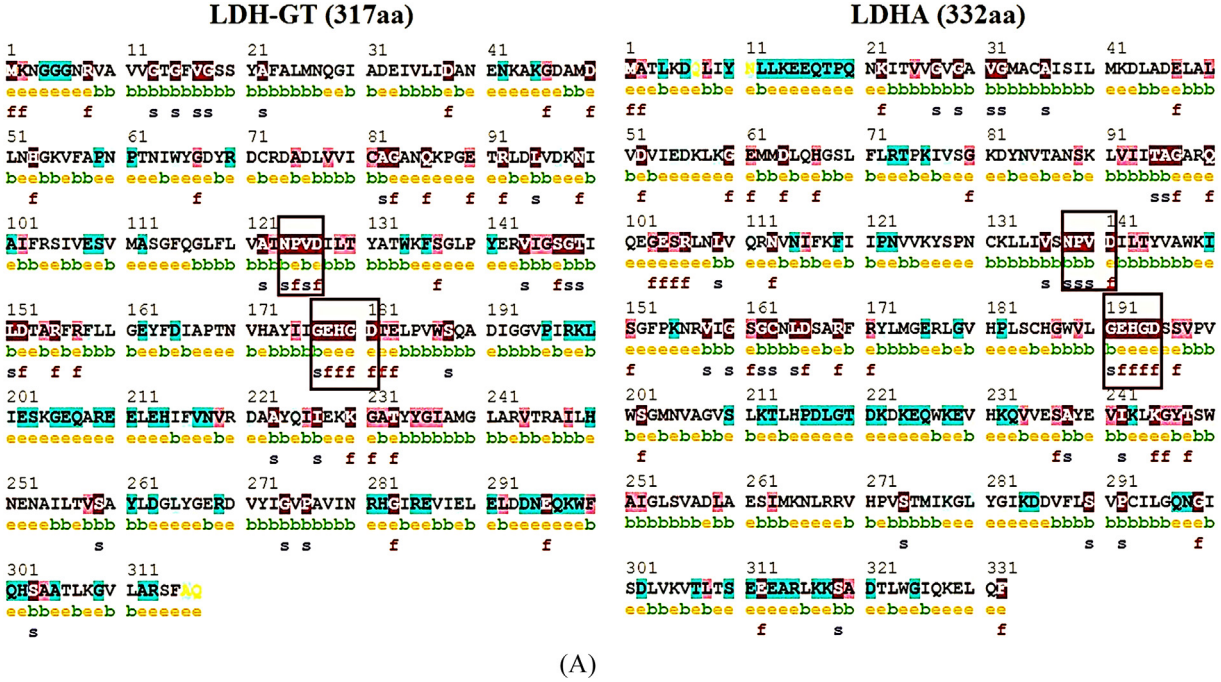

Fig. 7. A. ConSurf output showing conserved regions in maroon color and few identical residues batched of LDH-GT and LDHA (highlighted in maroon boxes); **e** indicates exposed residues; **b** refers to buried residues; **f** represents functional residues; and **s** refers to structural residues. **B.** The color-coded conservation scale of ConSurf output.

Financial support

This article was funded by the Deanship of Scientific Research (DSR) at King Abdulaziz University, Jeddah.

Acknowledgments

The authors acknowledge DSR for technical and financial support.

Supplementary material

Supplementary data to this article can be found online at https://doi.org/10.1016/j.ejbt.2018.06.003

References

[1] Burgner JW, Ray WJ. On the origin of the lactate dehydrogenase induced rate effect. Biochemistry 1984;23(16):3636–48. https://doi.org/10.1021/bi00311a010.
[2] Pineda JE, Callender R, Schwartz SD. Ligand binding and protein dynamics in lactate dehydrogenase. Biophys J 2007;93(5):1474–83. https://doi.org/10.1529/biophysj.107.106146.
[3] Valvona CJ, Fillmore HL, Nunn PB, et al. The regulation and function of lactate dehydrogenase A: Therapeutic potential in brain tumor. Brain Pathol 2016;26(1):3–17. https://doi.org/10.1111/bpa.12299.
[4] Kelly B, O'Neill LA. Metabolic reprogramming in macrophages and dendritic cells in innate immunity. Cell Res 2015;25(7):771–84. https://doi.org/10.1038/cr.2015.68.
[5] Brooks GA. Lactate shuttles in nature. Biochem Soc Trans 2002;30(2):258–64. https://doi.org/10.1042/0300-5127:0300258.
[6] Fiume L, Manerba M, Vettraino M, et al. Inhibition of lactate dehydrogenase activity as an approach to cancer therapy. Future Med Chem 2014;6(4):429–45. https://doi.org/10.4155/fmc.13.206.
[7] Di Stefano G, Manerba M, Di Ianni L, et al. Lactate dehydrogenase inhibition: Exploring possible applications beyond cancer treatment. Future Med Chem 2016;8(6):713–25. https://doi.org/10.4155/fmc.16.10.
[8] Kannan B, Jahanshahi-Anbuhi S, Pelton RH, et al. Printed paper sensors for serum lactate dehydrogenase using pullulan-based inks to immobilize reagents. Anal Chem 2015;87(18):9288–93. https://doi.org/10.1021/acs.analchem.5b01923.
[9] Garcia SO, Ulyanova YV, Figueroa-Teran R, et al. Wearable sensor system powered by a biofuel cell for detection of lactate levels in sweat. ECS J Solid State Sci Technol 2016;5(8):3075–81. https://doi.org/10.1149/2.0131608jss.
[10] Abraham MA, Rasti M, Bauer PV, et al. Leptin enhances hypothalamic lactate dehydrogenase A (LDHA)–dependent glucose sensing to lower glucose production in high-fat-fed rats. J Biol Chem 2018;293(11):4159–66. https://doi.org/10.1074/jbc.ra117.000838.
[11] Nikolaus N, Strehlitz B. Amperometric lactate biosensors and their application in (sports) medicine, for life quality and wellbeing. Microchim Acta 2008;160(1–2):15–55. https://doi.org/10.1007/s00604-007-0834-8.
[12] Zheng Y, Zhao X, Zhou J, et al. Identification of yak lactate dehydrogenase B gene variants by gene cloning. Sci China C Life Sci 2008;51(5):430–4. https://doi.org/10.1007/s11427-008-0036-6.
[13] Singh V, Kaushal DC, Rathaur S, et al. Cloning, overexpression, purification and characterization of *Plasmodium knowlesi* lactate dehydrogenase. Protein Expr Purif 2012;84(2):195–203. https://doi.org/10.1016/j.pep.2012.05.008.
[14] Nadeem MS, Moran J, Murtaza BN, et al. Cloning, *E. coli* expression, and characterization of heart lactate dehydrogenase B from river buffalo (*Bubalus bubalis*). Anim Biotechnol 2014;25(1):23–34. https://doi.org/10.1080/10495398.2013.804832.
[15] Weekes J, Yüksel GÜ. Molecular characterization of two lactate dehydrogenase genes with a novel structural organization on the genome of *Lactobacillus* sp. strain MONT4. Appl Environ Microbiol 2004;70(10):6290–5. https://doi.org/10.1128/aem.70.10.6290-6295.2004.
[16] Xia H, Wu C, Xu Q. Molecular cloning and characterization of lactate dehydrogenase gene 1 in the silkworm, *Bombyx mori*. Mol Biol Rep 2011;38(3):1853–60. https://doi.org/10.1007/s11033-010-0302-0.
[17] Erdemir A, Aktas M, Dumanli N, et al. Isolation, cloning and sequence analysis of lactate dehydrogenase gene from *Theileria annulata* may lead to design of new antitheilerial drugs. Vet Med 2012;57(10):559–67. https://doi.org/10.17221/6368-vetmed.
[18] Pagadala NS, Syed K, Tuszynski J. Software for molecular docking: A review. Biophys Rev 2017;9(2):91–102. https://doi.org/10.1007/s12551-016-0247-1.
[19] Corbeil CR, Williams CI, Labute P. Variability in docking success rates due to dataset preparation. J Comput Aided Mol Des 2012;26(6):775–86. https://doi.org/10.1007/s10822-012-9570-1.
[20] Venkatachalam CM, Jiang X, Oldfield T, et al. LigandFit: A novel method for the shape-directed rapid docking of ligands to protein active sites. J Mol Graph Model 2003;21(4):289–307. https://doi.org/10.1016/s1093-3263(02)00164-x.
[21] Allen WJ, Balius TE, Mukherjee S. DOCK 6: Impact of new features and current docking performance. J Comput Chem 2015;36(15):1132–56. https://doi.org/10.1002/jcc.23905.
[22] Laemmli UK. Cleavage of structural proteins during the assembly of the head of bacteriophage T4. Nature 1970;227(5259):680. https://doi.org/10.1038/227680a0.
[23] Biasini M, Bienert S, Waterhouse A, et al. SWISS-MODEL: Modelling protein tertiary and quaternary structure using evolutionary information. Nucleic Acids Res 2014;42(W1):252–8. https://doi.org/10.1093/nar/gku340.
[24] Yang J, Zhang Y. I-TASSER server: New development for protein structure and function predictions. Nucleic Acids Res 2015;43(W1):174–81. https://doi.org/10.1093/nar/gkv342.
[25] Lovell SC, Davis IW, Arendall WB. Structure validation by Cα geometry: ϕ, ψ and Cβ deviation. Proteins Struct Funct Genet 2003;50(3):437–50. https://doi.org/10.1002/prot.10286.
[26] Shi Y, Pinto BM. Human lactate dehydrogenase A inhibitors: a molecular dynamics investigation. PLoS One 2014;9(1):e86365. https://doi.org/10.1371/journal.pone.0086365.
[27] Macindoe G, Mavridis L, Venkatraman V, et al. HexServer: an FFT-based protein docking server powered by graphics processors. Nucleic Acids Res 2010;38:445–9. https://doi.org/10.1093/nar/gkq311.
[28] Celniker G, Nimrod G, Ashkenazy H. ConSurf: using evolutionary data to raise testable hypotheses about protein function. Isr J Chem 2013;53(3–4):199–206. https://doi.org/10.1002/ijch.201200096.
[29] Ashkenazy H, Abadi S, Martz E. ConSurf 2016: An improved methodology to estimate and visualize evolutionary conservation in macromolecules. Nucleic Acids Res 2016;44:W1):44–350. https://doi.org/10.1093/nar/gkw408.
[30] Le A, Cooper CR, Gouw AM, et al. Inhibition of lactate dehydrogenase A induces oxidative stress and inhibits tumor progression. Proc Natl Acad Sci U S A 2010;107(5):2037–42. https://doi.org/10.1073/pnas.0914433107.
[31] Michels H, Seinstra RI, Uitdehaag JC, et al. Identification of an evolutionary conserved structural loop that is required for the enzymatic and biological function of tryptophan 2,3-dioxygenase. Sci Rep 2016;6(1):39199. https://doi.org/10.1038/srep39199.
[32] Walker SS, Labroli M, Painter RE. Antibacterial small molecules targeting the conserved TOPRIM domain of DNA gyrase. PLoS One 2017;12(7):e0180965. https://doi.org/10.1371/journal.pone.0180965.
[33] Francis DM, Page R. Strategies to optimize protein expression in *E. coli*. Curr Protoc Protein Sci 2010;29:5–24. https://doi.org/10.1002/0471140864.ps0524s61.
[34] Abraham N, Paul B, Ragnarsson L, et al. *Escherichia coli* protein expression system for acetylcholine binding proteins (AChBPs). PLoS One 2016;11(6):e0157363.31. https://doi.org/10.1371/journal.pone.0157363.
[35] Yeswanth S, Kumar YN, Prasad UV, et al. Cloning and characterization of L-lactate dehydrogenase gene of *Staphylococcus aureus*. Anaerobe 2013;24:43–8. https://doi.org/10.1016/j.anaerobe.2013.09.003.
[36] Al-Jassabi S. Purification and kinetic properties of skeletal muscle lactate dehydrogenase from the lizard *Agama stellio stellio*. Biochemistry (Moscow) 2002;67(7):786–9. https://doi.org/10.1023/A:1016300808378.
[37] Wang Y, Wei L, Wei D, et al. Enzymatic kinetic properties of the lactate dehydrogenase isoenzyme C4 of the Plateau Pika (*Ochotona curzoniae*). Int J Mol Sci 2016;17(1):39. https://doi.org/10.3390/ijms17010039.
[38] Ozkan M, Yllmaz EI, Lynd LR, et al. Cloning and expression of the *Clostridium thermocellum* L-lactate dehydrogenase gene in *Escherichia coli* and enzyme characterization. Can J Microbiol 2004;50(10):845–51. https://doi.org/10.1139/w04-071.
[39] Talaiezadeh A, Shahriari A, Tabandeh MR, et al. Kinetic characterization of lactate dehydrogenase in normal and malignant human breast tissues. Cancer Cell Int 2015;15(1):19. https://doi.org/10.1186/s12935-015-0171-7.
[40] Arnold K, Bordoli L, Kopp J, et al. The SWISS-MODEL workspace: A web-based environment for protein structure homology modelling. Bioinformatics 2006;22(2):195–201. https://doi.org/10.1093/bioinformatics/bti770.
[41] Delano W. The PyMOL molecular graphics system. San Carlos, CA: DeLano Scientific; 2002 [cited September 2010]. Available from Internet http://www.ccp4.ac.uk/newsletters/newsletter40/11_pymol.pdf.
[42] Zeng Y, Wang Y, Yu Z, et al. Hypersensitive response of plasmid-encoded AHL synthase gene to lifestyle and nutrient by *Ensifer adhaerens* X097. Front Microbiol 2017;8(1160). https://doi.org/10.3389/fmicb.2017.01160.
[43] Mohammad N, Karsabet MT, Amani J, et al. *In silico* design of a chimeric protein containing antigenic fragments of *Helicobacter pylori*; a bioinformatic approach. Open Microbiol J 2016;10(97). https://doi.org/10.2174/1874285801610010097.